Electronic Supplementary Information (ESI)

Non-activation MOF arrays as coating layer to fabricate stable superhydrophobic micro/nano flower-like architecture

Guoliang Zhang, *, [a] Jiaheng Zhang, [a] Pengcheng Su, [a] Zehai Xu, [a] Wanbin Li, [a] Chong Shen [b] and Qin Meng *, [b]

[a] *Institute of Oceanic and Environmental Chemical Engineering, State Key Lab Breeding Base of Green Chemical Synthesis Technology, Zhejiang University of Technology, Chaowang Road 18#, Hangzhou, Zhejiang 310014, China*

Tel/Fax: 86-571-88320863

[b] *College of Chemical and Biological Engineering, State Key Laboratory of Chemical Engineering, Zhejiang University, 38 Zheda Road, Hangzhou, Zhejiang 310027, China*

Tel/Fax: 86-571-87953193

**Corresponding author E-mail: guoliangz@zjut.edu.cn*

**Co-Corresponding author E-mail: mengq@zju.edu.cn*

Contents

1. Experimental Detail

1.1 Materials

The commercial copper mesh (200 meshes per inch) was purchased from local hardware store. Zinc nitrate hexahydrate (99.0%), toluene (≥99.5%) and dichloromethane (≥99.5%) were purchased from Changzheng Chemical Reagent Co., China. Sodium formate (99.5%), n-hexane, petroleum ether (bp 60-90°C), 2-methylimidazole (98%) and benzimidazole (>98.0%) were supplied by Hangzhou Banghua Chemical Co., China. Soybean oil was purchased from supermarket. The solvents of methanol anhydrous (≥99.5%) and N,N-dimethylformamide (DMF, ≥99.5%) were used as received without further purification. The water used in this study was obtained from a RO-EDI system. The ion concentrations were measured by IRIS Intrepid ICP and Metrohm 861 Compact IC, which were controlled to meet $\sigma \leq 0.5$ μS cm^{-1}.

1.2 Methods

Preparation of ZnO array coatings. Briefly, the solid of zinc nitrate hexahydrate (0.59g), 2-methylimidazole (0.245g) and sodium formate (0.135g) were dissolved in 16 ml methanol by ultrasound. The copper mesh was cleaned ultrasonically in methanol anhydrous and then the cleaned copper mesh was immersed vertically in the solution which contained in a Teflon lined stainless steel autoclave. The autoclave was heat-treated at 80 °C for 12h. After cooling to room temperature, the obtained ZnO array coatings were rinsed with methanol for several times and dried at atmosphere.

Preparation of superhydrophobic ZIF-7 array coatings. To obtain ZIF-7 array coatings, 0.245g benzimidazole was dissolved in 16ml DMF. The prepared ZnO arrays were taken as the metal source for the synthesis of ZIF-7 array coatings. ZnO array coatings were uprightly placed in a Teflon lined stainless steel autoclave. Then the solution of ligand was transferred to the autoclave, followed by heating at 150 °C for 12h for ZIF-7 growth. After the ligand-solvothermal reaction, the as-synthesized ZIF-7 array coatings were taken out, naturally cooled to room temperature and washed with

DMF for several times, and then dried in air. For comparison, the ZIF-7 growing directly on copper mesh was also prepared by dissolving zinc nitrate hexahydrate (0.283g) and benzimidazole (0.161g) in 16ml DMF and heat-treated at 130 °C for 48h.

Preparation of ZIF-8 array coatings. 2-methylimidazole (0.245g) was dissolved in methanol (16 ml). Consistent with the synthesis of ZIF-7 array coatings, the ZnO array coatings were transferred into Teflon lined stainless steel autoclave and then immersed in the solution. After that, the autoclave was subjected to heat-treatment at 80 °C for 24h. After cooling to room temperature, the obtained ZIF-8 array coatings were washed with methanol for several times and dried at atmosphere.

1.3 Thermal stability test of prepared MOF array coatings

The prepared MOF array coatings were calcined at various temperatures using an Electrical Resistance Furnace (YFX 7/100-6C, SHANGHAI Y-FENG CO., China) in air atmosphere. In the heat-treated progress, temperature-programmed route was used at a heating rate of 5 °C min^{-1} and samples were heat-treated 2h at the specified temperatures. After that, the MOF array coatings cooled to room temperature naturally. In addition, the performance parameters of the MOF array coatings which had already been annealing treatment were tested by SEM, XRD and water contact angle.

1.4 Efficiency in oil-water separation

To study the oil-water separation performance of the ZIF-7 array coatings, a simple effective filtration experiment by gravity was designed. The as-prepared super-hydrophobic ZIF-7 array coatings were sealed between two plastic tubes. A mixture of oil (toluene, n-hexane, petroleum ether, soy-bean oil and dichloromethane) and water (50% v/v) were poured slowly onto ZIF-7 array coatings. And then the oil spontaneously permeated quickly. The water was dyed by methylene blue for easy observation. The oil-water separation procedure was driven simply by gravity. The finally obtained filtrate was collected for absorbance tests. Here the separation efficiency (SE) is calculated as follows:

$$SE = (A_0 - A_1)/A_0 \times 100\% \quad (1)$$

where A_0 is the absorbance of original solution, and A_1 is the absorbance of the filtrate.

1.5 Characterization of structure and hydrophobicity

The morphologies of ZIF-7 array coatings were inspected by scanning electron microscopy (SEM, TM-1000, Hitachi, Japan). X-ray diffraction (XRD) patterns of all samples were recorded using an X'Pert PRO (PNAlytical, Netherlands) diffractometer in the reflection mode with CuKα radiation (40kV, 40mA, λ=0.154056 nm). For surface component analysis, the FT-IR spectra were measured with a spectrometer (Nicolet 6700, Thermo Scientific, USA) in the range 4000-400 cm^{-1}. Water contact angle and sliding angle of the different samples were measured by using an optical contact angle meter (Dataphysics OCA30, Germany) at ambient temperature. For contact angle, 4μL water droplets were used and the contact angle of the water droplet was directly observed after 4s. 10μL water droplet was employed for sliding angle tests. The absorbance of filtrate was determined by Vis Spectrophotometer (722s, Lengguang, China).

2. Results and Discussions

2.1 Characterization:

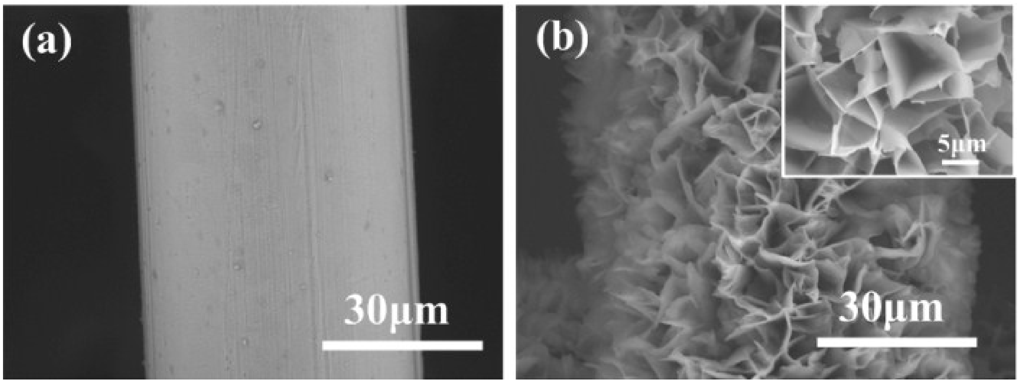

Fig. S1 SEM images of (a) initial copper mesh and (b) flake-like ZnO array coatings.

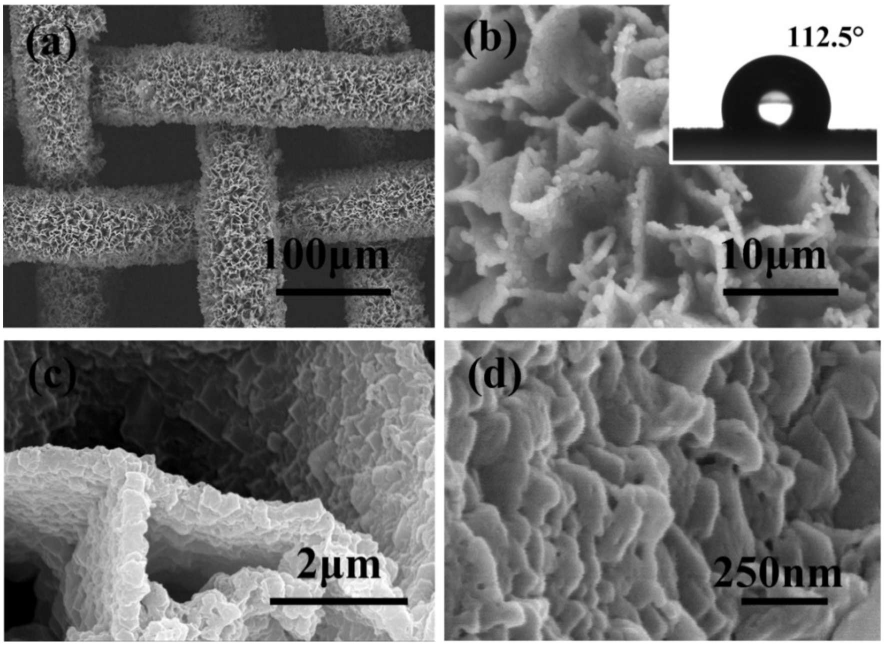

Fig. S2 The structure characteristics of ZIF-8 array coatings. (a) Low-magnification SEM image of ZIF-8 array coatings. (b)(c)(d) High-magnification SEM images of ZIF-8 array coatings.

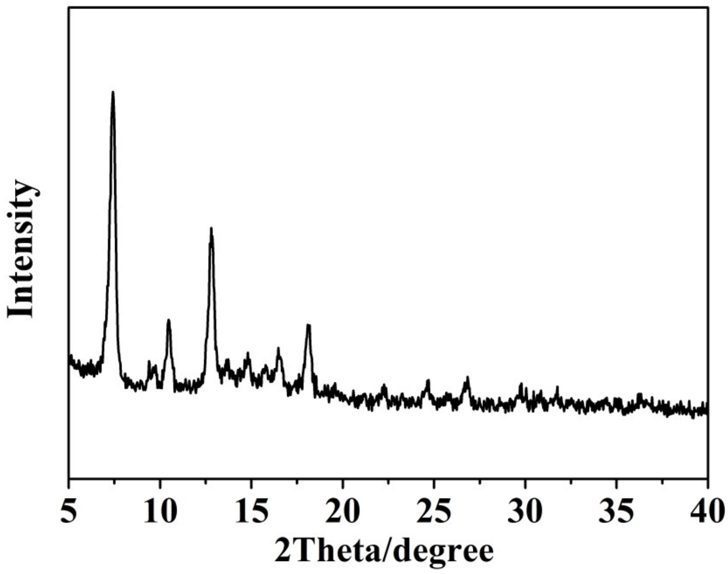

Fig. S3 XRD patterns of synthesized ZIF-8 array coatings.

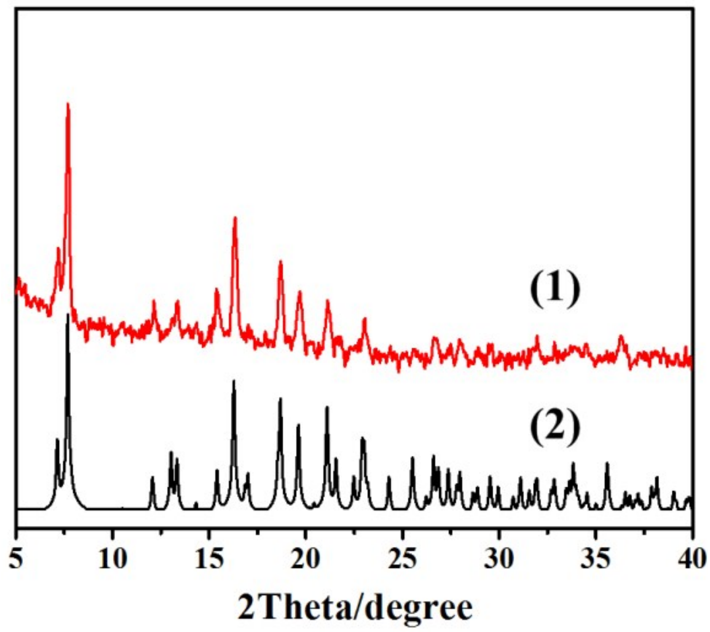

Fig. S4 XRD patterns of (1) as-prepared ZIF-7 array coatings and (2) simulated ZIF-7.

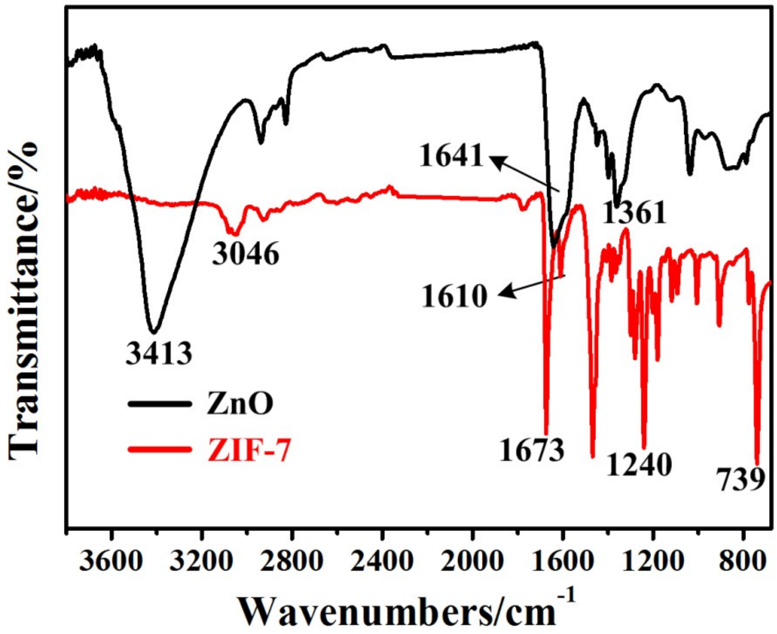

Fig. S5 FTIR of the ZnO and ZIF-7 array coatings.

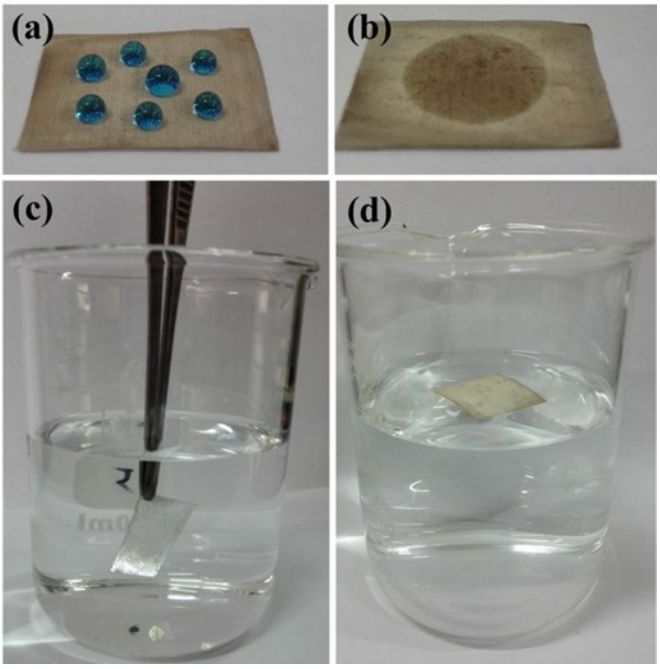

Fig. S6 The optical images of (a) water droplets and (b) an oil droplet on the super-hydrophobic ZIF-7 array coatings; (c) ZIF-7 array coatings were immersed in water by an external force; (d) Picture of ZIF-7 array coatings floating on the water. The optical images also show that the water droplets can stand on the surface of the ZIF-7 array coatings and keep an almost complete sphere, while oil droplets can permeate rapidly and the contact angle of the oil droplets is nearly zero. Furthermore, a mirror-like surface can be observed when the superhydrophobic ZIF-7 array coating was pressed into water, proving that there was trapped air at the surface of the ZIF-7 array coatings. The ZIF-7 array coatings floated freely on the water like a boat when the external force was withdrawn. After removing the ZIF-7 array coatings from the water, no water was found to adhere to the surface. The outstanding superhydrophobicity can be ascribed to the hierarchical micro/nanoscale structure of the MOF array coatings and the intrinsic hydrophobicity of ZIF-7.

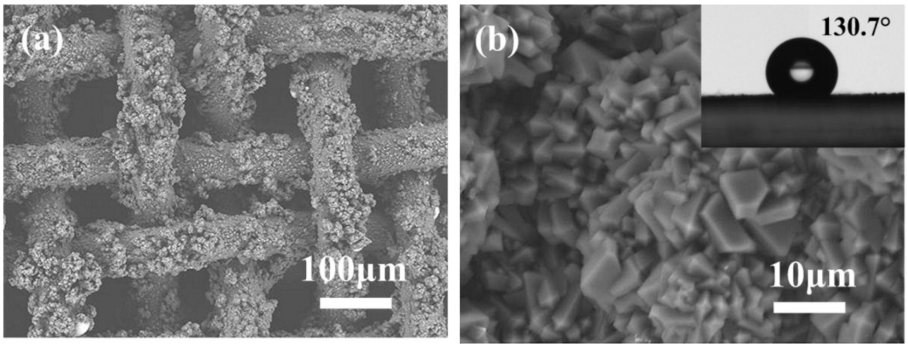

Fig. S7 SEM images of (a) ZIF-7 growing directly on the substrate, (b) high magnifications. The inset is water contact angle of corresponding sample.

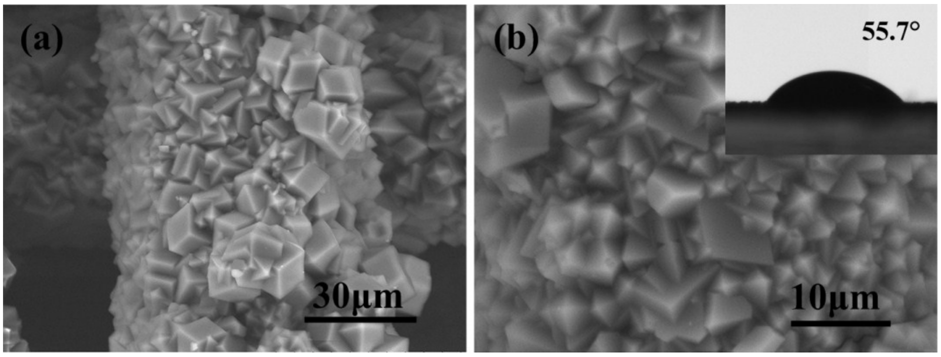

Fig. S8 SEM images of (a) ZIF-8 growing directly on the substrate, (b) high magnifications. The inset is water contact angle of corresponding sample.

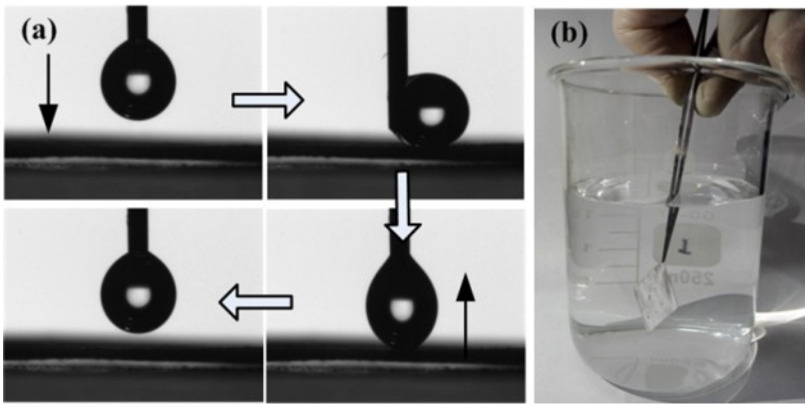

Fig. S9 (a) Dynamic water repelling processes on the surface of ZIF-7-300; (b) ZIF-7-300 was immersed in water by an external force.

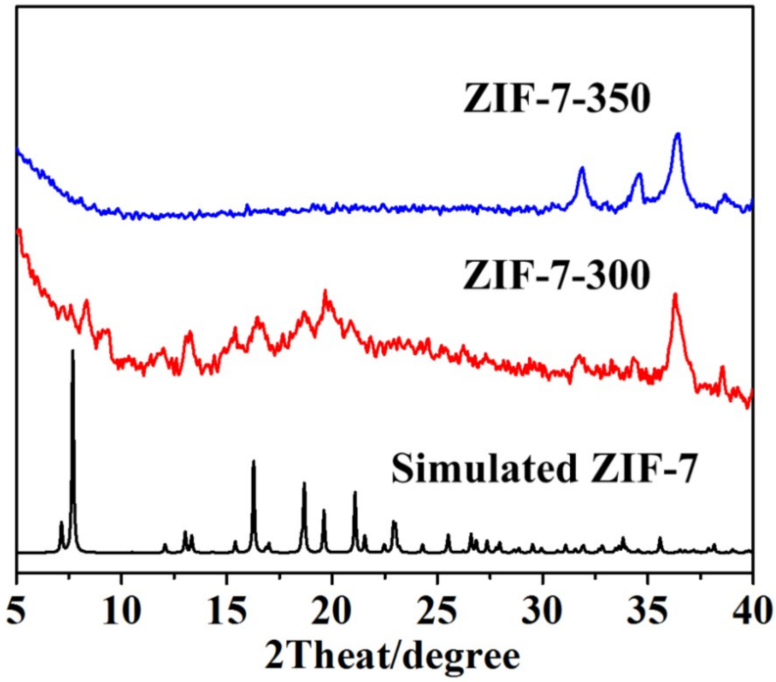

Fig. S10 XRD patterns of ZIF-7-300, ZIF-7-350 and the simulated ZIF-7.

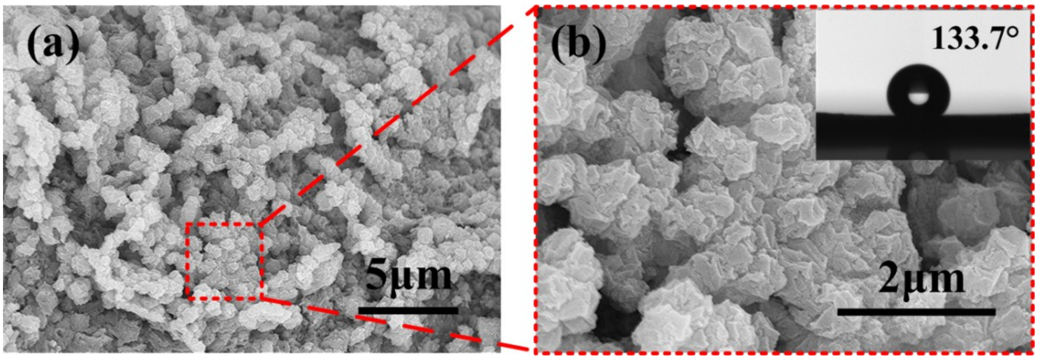

Fig. S11 SEM images of (a) ZIF-7-350 and (b) high magnifications. The inset is water contact angle of corresponding sample.

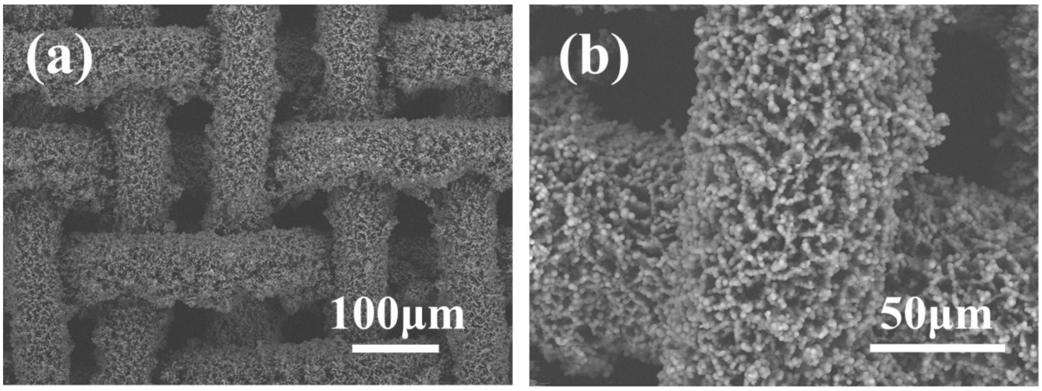

Fig. S12 SEM images of (a)(b) ZIF-7 array coatings after oil/water separation, (b) high magnifications.

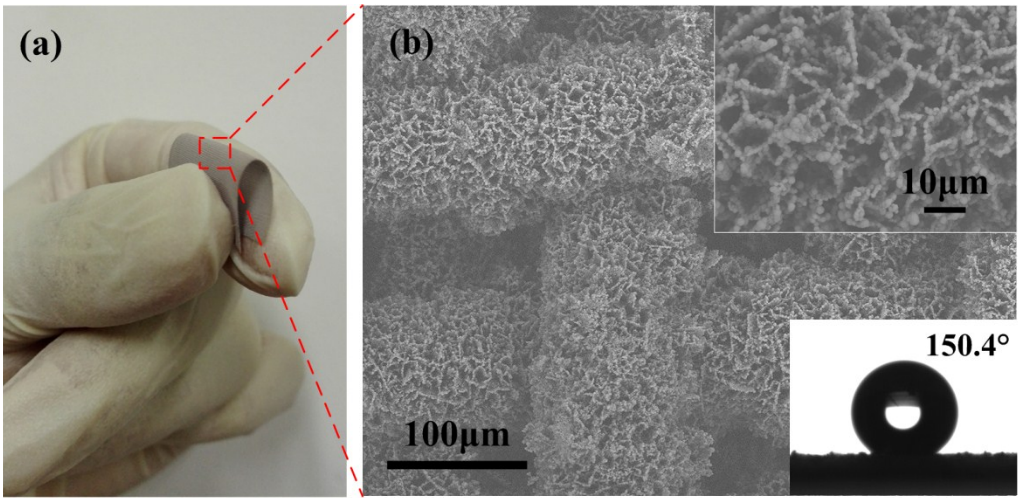

Fig. S13 Qualitative test of mechanical stability by multiple-bending tests. (a) the scheme of bending tests, (b) SEM images of the corresponding places, the insets are high magnification image and water contact angle.

2.2 Comparisons of ZIF array coatings with other MOF materials

Table S1. Comparisons of ZIF array coatings with other MOF materials

MOF	**Chemical modification type**	**Investigated Form**	**Contact angle[°]**	**Ref.**
FMOF-1	Fluorinated aromatic ring	powder	no water molecules can enter into voids	S1
MOFF-1	Fluorinated aromatic ring	pressed crystals	108±2	S2
MOFF-2	Fluorinated aromatic ring	pressed crystals	151±1	
MOFF-3	Fluorinated aromatic ring	pressed crystals	135±2	
ZIF-90	Fluorinated aromatic ring	particle	152.4	S3
NH_2-MIL-53(Al)	perfluorooctanoyl chloride	mushroom caps coated AAO membrane	151-169	S4
UHMOF-100	Fluorinated aromatic linker	desolvated crystalline powder	176	S5
NMOF-1	alkyl chain (OPE-C_{18})	coated glass substrates	160-162	S6
PESD-1	aromatic ring	single crystal	>150	S7
		powder	>150	
		powder	>150	
		pellet disk (5 MPa)	ca.110	
MIL-53(Al)-AM4	alkyl chain (C_4)	Powder	>150	S8
MIL-53(Al)-AM6	alkyl chain (C_6)	Powder		
ZIF-7	NA	array coatings on mesh	151.3	This work
ZIF-7-300	NA	array coatings on mesh	154.7	

2.3 Comparisons on the separation performance of the ZIF array coatings with other superhydrophobic materials

Table S2. Comparisons on the separation performance of the ZIF array coatings with other superhydrophobic materials

Oil/water separation materials	Water Contact angle (°)	Separation or absorption substances	Separation efficiency (%) or Absorption capacities (times)	Recyclability (times)	Ref.
Graphdiyne-Based Foam	160.1	dichloromethane	>98%	Good	S9
Cu_2O nanorods on copper meshes	162±1.4	n-hexane, gasoline, diesel oil, toluene, chloroform	>96%	10	S10
pDA coatings	162	crude oil	97.1%	n.a.	S11
GT Fabric	151	n-hexane, dodecane, hexadecane, chloroform	99.2%	n.a.	S12
PET textiles	156.5-166.7	n-hexane, diesel oil, crude oil, sunflower seed oil	>97%	Good	S13
ZnO nanorod-coated mesh	157±1	Gasoline, petroleum ether, hexane, diesel	92-97.5%	n.a.	S14
PVDF membranes	158	Water-in-oil emulsions (including surfactant-free and surfactant-stabilized emulsions)	>99.95%	20	S15
ZnO/PDMS coated mesh	151-158	n-hexane, motor oil, paraffin liquid, vegetable oil, crude oil,	>94%	10	S16
PDVB-modified mesh	154.8	gasoline, diesel, n-hexane, lubrication oil, toluene	>99.99%	30	S17
N-TESPS fiberglass fabrics	154.8	hexane, chloroform, kerosene, gas oil	>98%	30	S18
DLC-coated cotton textile	169.3±2.2	gasoline, pump oil, fats, organic solvents	1.25-14 times	6	S19
MTMS-DMDMS gels	152.6	n-hexane, chloroform, mineral oil, toluene, petroleum ether, et al.	6.2-14 times	10	S20

PODS-modified sponge	153	toluene, light petroleum, methylsilicone oil	42-68 times	50	S21
Sponge@HFGO@ZIF-8	162	petroleum ether, silicone oil, chloroform, coconut oil, deca octane oil, veg oil	1.5-6 times	n.a.	S22
ZIF-7 array coatings ZIF-7-300 array coatings	151.3 154.7	toluene, n-hexane, petroleum ether, soybean oil, dichloromethane	97-99.9%	10	This work

3. Reference

(S1) C. Yang, U. Kaipa, Q. Z. Mather, X. Wang, V. Nesterov, A. F. Venero, M. A. Omary, *J. Am. Chem. Soc.* 2011, **133**, 18094-18097.

(S2) T. Chen, I. Popov, O. Zenasni, O. Daugulis, O. S. Miljanic, *Chem. Commun.* 2013, **49**, 6846-6848.

(S3) C. Liu, Q. Liu, A. Huang, *Chem. Commun*. 2016, **52**, 3400-3402.

(S4) T. T. Y. Tan, M. R. Reithofer, E. Y. Chen, A. G. Menon, T. S. A. Hor, J. Xu, J. M. Chin, *J. Am. Chem. Soc*. 2013, **135**, 16272-16275.

(S5) S. Mukherjee, A. M. Kansara, D. Saha, R. Gonnade, D. Mullangi, B. Manna, A. V. Desai, S. H. Thorat, P. S. Singh, A. Mukherjee, S. K. Ghosh, *Chem. Eur. J*. 2016, **22**, 10937-10943.

(S6) S. Roy, V. M. Suresh, T. K. Maji, *Chem. Sci.* 2016, **7**, 2251-2256.

(S7) K. P. Rao, M. Higuchi, K. Sumida, S. Furukawa, J. Duan, S. Kitagawa, *Angew. Chem. Int. Ed.* 2014, **53**, 8225-8230.

(S8) J. G. Nguyen, S. M. Cohen, *J. Am. Chem. Soc.* 2010, **132**, 4560-4561.

(S9) X. Gao, J. Zhou, R. Du, Z. Xie, S. Deng, R. Liu, Z. Liu, J. Zhang, *Adv. Mater.* 2016, **28**, 168-173.

(S10) L. Kong, X. Chen, L. Yu, Z. Wu, P. Zhang, *ACS Appl. Mater. Interfaces* 2015, **7**, 2616-2625.

(S11) Z. Wang, Y. Xu, Y. Liu, L. Shao, *J. Mater. Chem. A* 2015, **3**, 12171-12178.

(S12) Y. Liu, X. Wang, B. Fei, H. Hu, C. Lai, J. Xin, *Adv. Funct. Mater.* 2015, **25**, 5047-5056.

(S13) C. Xue, Y. Li, J. Hou, L. Zhang, J. Ma, S. Jia, *J. Mater. Chem. A* 2015, **3**, 10248-10253.

(S14) H. Li, Y. Li, Q. Liu, *Nanoscale Res. Lett.* 2013, **8**, 183.

(S15) W. Zhang, Z. Shi, F. Zhang, X. Liu, J. Jin, L. Jiang, *Adv. Mater.* 2013, **25**, 2071-2076.

(S16) G. Wang, Z. Zeng, H. Wang, L. Zhang, X. Sun, Y. He, L. Li, X. Wu, T. Ren, Q. Xue, *ACS Appl. Mater. Interfaces* 2015, **7**, 26184-26194.

(S17) W. Zhang, N. Liu, Y. Cao, Y. Chen, L. Xu, X. Lin, L. Feng, *Adv. Mater.* 2015, **27**, 7349-7355.

(S18) A. Rostami, S. Sharifnia, *J. Mater. Chem. A* 2017, **5**, 680-688.

(S19) B. Cortese, D. Caschera, F. Federici, G. M. Ingoc, G. Gigli, *J. Mater. Chem. A*

2014, **2**, 6781-6789.

(S20) G. Hayase, K. Kanamori, M. Fukuchi, H. Kaji, K. Nakanishi, *Angew. Chem. Int. Ed.* 2013, **52**, 1986-1989.

(S21) Q. Ke, Y. Jin, P. Jiang, J. Yu, *Langmuir* 2014, **30**, 13137-13142.

(S22) K. Jayaramulu, K. K. R. Datta, C. Rçsler, M. Petr, M. Otyepka, R. Zboril, R. A. Fischer, *Angew. Chem. Int. Ed.* 2016, **55**, 1178-1182.